Field Emission Testing of Carbon Nanotubes for THz Frequency Vacuum Micro-Tube Sources

Harish Manohara[1], Wei Lien Dang[2], Peter H. Siegel[1], Michael Hoenk[1], Ali Husain[2], Axel Scherer[2]

[1]Jet Propulsion Laboratory, 4800 Oak Grove Drive, California Institute of Technology, Pasadena, CA 91109;
[2]Department of Electrical Engineering, California Institute of Technology, 1200 E. California Blvd., Pasadena, CA 91125

ABSTRACT

A carbon nanotube-based high current density electron field emission source is under development at Jet Propulsion Laboratory (JPL) for submillimeter-wave power generation (300 GHz to 3 THz). This source is the basis for a novel vacuum microtube component: the *nanoklystron*. The nanoklystron is a monolithically fabricated reflex klystron with dimensions in the micrometer range. The goal is to operate this device at much lower voltages than would be required with hot-electron sources and at much higher frequencies than have ever been demonstrated. Both single-walled (SWNTs) as well as multi-walled nanotubes (MWNTs) are being tested as potential field-emission sources. This paper presents initial results and observations of these field emission tests. SWNTs and MWNTs were fabricated using standard CVD techniques. The tube density was higher in the case of MWNT samples. As previously reported, high-density samples suffered from enhanced screening effect thus decreasing their total electron emission. The highest emission currents were measured from disordered, less dense MWNTs and were found to be ~0.63 mA @ 3.6 V/μm (sample 1) and ~3.55 mA @ 6.25 V/μm (sample 2). The high density vertically aligned MWNTs showed low field emission as predicted: 0.31 mA @ 4.7 V/μm.

Keywords: Nanoklystron, Field emission, Nanotubes, THz sources, SWNT, MWNT

1. INTRODUCTION

1.1 Carbon nanotubes as field emitters

The commercial interest in flat panel display technology has engendered much research on the fabrication and characterization of nanostructured materials for field emission applications[1,2]. Low cost fabrication over large areas has proven to be an elusive goal, particularly for applications that demand large emission current (which demands, in turn, robust emitter materials). Not surprisingly, carbon nanotubes have been found to be promising as a low-cost, robust, nanostructured material, and prototype field emission displays based on carbon nanotubes have been reported in the literature[3]. Electron field emission has been demonstrated from both multi-walled carbon nanotubes (MWNTs) as well as single-walled carbon nanotubes (SWNTs). The small diameter of carbon nanotubes (diameter of a single SWNT can be ~ 1 nm) enables efficient emission at low fields, despite their relatively high work function (> 4.5eV). At 1-3 V/μm of threshold fields, carbon nanotubes are the best suited for low-power, high-current density applications. A comparison of nanostructured carbon cold cathodes[4] concluded that carbon nanotubes are more robust than diamond, with the ability to deliver current densities in excess of 1 A/cm^2. Intriguingly, the authors of this study have speculated that achievable current densities with carbon nanotubes might be orders of magnitude higher, based on the ability of a single carbon nanotube to emit 30 nA[5].

The emitted current from a field emitter depends directly upon the local electric field at the emitting surface and can be simply modeled by the Fowler-Nordheim relationship[6]. A consequence of this is that very small variations in the emitter geometry and surface conditions can have marked effects on the emitted current. Alignment, purification, end type (open or closed), density and spacing of tubes are the primary variables to the amount of electron current that can be produced[2]. CNT field emitters for space applications will require not only minimizing the size and power consumption of these devices, but also minimizing the voltage required for a sufficient electron current. This end can be achieved through the use of an integrated extraction grid. Previous work has shown that reducing the separation of the grid anode from the CNT emitters rapidly reduces the voltage required for a particular current[7]. However, a lot more work is required to achieve the level of uniformity, brightness, and stability required for high-current density applications. One such application being developed at the Jet Propulsion Laboratory (JPL) is a novel local oscillator source of terahertz (THz) radiation for high-resolution heterodyne spectroscopy. This device requires high-current density field emission source capable of delivering hundreds to a kA/cm^2. This paper concerns with the work in progress for achieving such high-current densities using carbon nanotubes.

1.2 Nanoklystron

The nanoklystron[8, 9] is a monolithically fabricated reflex klystron with dimensions in the micrometer range. The goal is to operate this device at much lower voltages (tens of volts) than would be required with hot-electron sources and generate milliwatts of power at much higher frequencies (300 GHz to 3 THz) than has ever been demonstrated. Figure 1 shows a conceptual sketch of a nanoklystron. In principle, the electrons
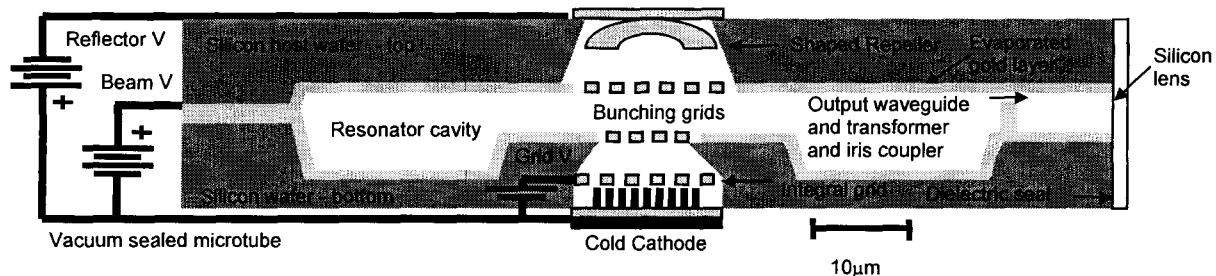

Fig. 1. Schematic cross section of a proposed nanoklystron. The cathode is composed of a carbon nanotube field emitter array with integrated grid. The cavity, beam and output waveguide are etched from two silicon wafers, which are later joined by bonding. The repeller and cathode are drop-in parts and vacuum sealing is performed in the last step.
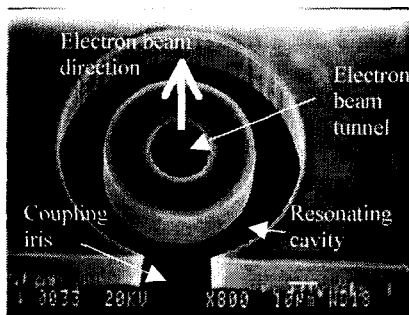

Fig. 2. SEM micrograph of the bottom half of a nanoklystron showing the cavity, iris and the electron beam tunnel. The beam tunnel diameter is ~ 20 μm.

generated at the source are made to traverse the gap between the electron beam tunnel and the repeller. As they travel the gap, the noise voltage in the device coupled with the repeller voltage causes density modulation of the beam resulting in bunching of electrons. When the conditions are right, the tube spontaneously bursts into oscillations generating power at frequencies dictated by the dimensions of the resonating cavity. This power is then coupled to the outside through a step waveguide transformer and a feedhorn. The frequency of operation of such a klystron is inversely proportional to the dimensions of the cavity, as a result, at THz frequencies the cavity is in the micrometer range requiring micromachining techniques for fabrication. Using multi-step lithography and deep-reactive ion etching (DRIE) techniques nanoklystrons of 0.3 THz, 0.6 THz and 1.2 THz have been fabricated monolithically in silicon. The cavity is fabricated in two

halves and the circuit area is coated with 250-nm thick gold layer. The two halves are then thermocompression bonded at 450° C and 2000 N piston force. Figure 2 shows the close-up view of the electron beam tunnel as it opens into the cavity. The tunnel is ~ 20 μm in diameter. With such small dimensions, the current density requirement of an electron source for this device can only be satisfied using a field emission source.

2. FIELD EMISSION TESTS

2.1 Carbon nanotube synthesis

High quality, single walled nanotubes (SWNTs) are grown by methane chemical vapor deposition (CVD) method employing an iron nitrate in isopropanol solution catalyst (see Fig. 3 (a)). The solution was spun onto the silicon substrates, which were previously dipped in hydrofluoric acid. The tubes were grown in a tube furnace with temperatures approaching 950° C as methane and hydrogen were flowed over the surface. For longer tubes the growth period was about 10 to 15 minutes and they measured ~ 5 nm in diameter. MWNTs were grown using a plasma-enhanced CVD process on patterned silicon and silicon dioxide substrates at temperatures below 600° C (see Figure 3 (b) and (c)). The process has been demonstrated with evaporated and sputtered metal catalysts, and with metal salt solutions spin-coated on silicon

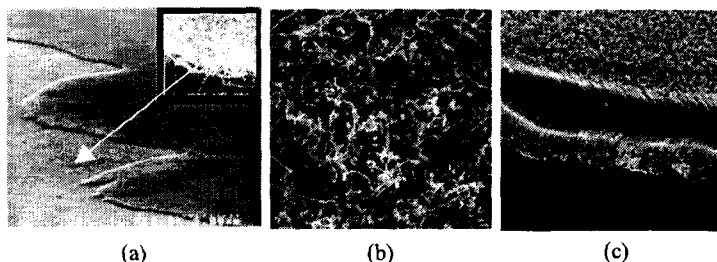(a)   (b)   (c)

Fig. 3. (a) SWNTs in a patterned region, (b) disordered, low-density random MWNTs, (c) vertically aligned, highly dense MWNTs

wafers. Some control is demonstrated over nanotube size and spacing, which affect field emission characteristics. MWNTs have been grown on planar samples of up to three inches in diameter, and the CVD process is scalable to still larger sample sizes. One advantage of chemical vapor deposition is that the growth is not limited to planar substrates, nor does it require a line-of-sight path between the source and the sample[10].

2.2 Sample Preparation

All of the field emission tests were conducted in a diode mode. A test template was fabricated for this purpose using micromachining (see Fig. 4 (a)). On a 5 mm by 5 mm square die of degenerately doped silicon ($\rho < 10^{-3}$ Ω-cm) substrate with ~ 1.5-μm thick oxide layer, a 3-mm diameter trench of ~ 10 μm depth was etched using DRIE. Using the photoresist-masking layer for DRIE as the sacrificial layer, catalyst metal was selectively deposited inside the trench and the nanotubes were grown as described in the previous sub-section (actual sample area was ~ 7 mm²). In case of SWNTs, the tubes stayed well below the surface, but in case of MWNTs, the tubes grown were dense and protruded, in some instances > 20 μm above the trench top. In such samples, extra thickness shims were used as spacers during the field emission test.

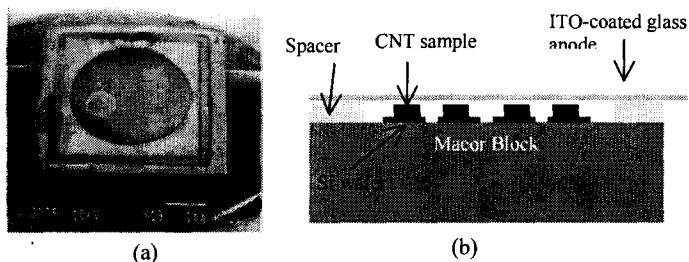

(a)   (b)

Fig. 4. (a) Carbon nanotube sample template (3-mm diameter trench is the CNT area), (b) Schematic of the measurement set-up inside a high vacuum chamber
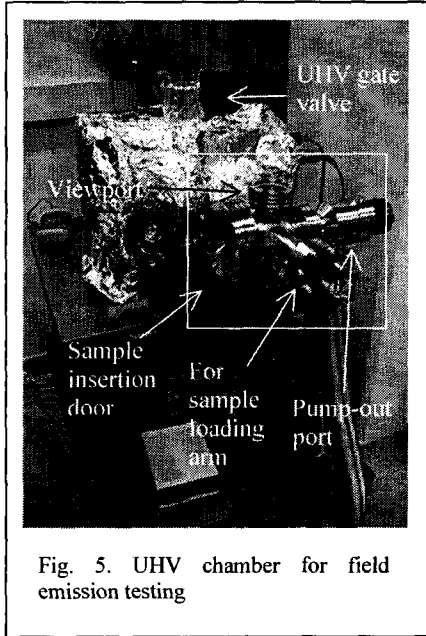
Fig. 5. UHV chamber for field emission testing

Multiple samples were attached to a highly flat machineable ceramic block, although MWNTs and SWNTs were tested in separate trials. Additional shims were used as spacers where necessary thus bringing the anode to cathode gap to a range of 40 μm to 160 μm. An Indium-Tin-Oxide (ITO) coated transparent glass slide was used as the anode. In order to identify the emission spots, the conductive side was coated with P-22 blue-pigmented phosphor (silver activated zinc sulfide) powder. Figure 4 (b) shows the schematic of the test setup. The setup was then loaded into a high vacuum chamber shown in Figure 5. The field emission tests were conducted at vacuums in the range of 10^{-6} Torr. This is one of the greatest advantages of carbon nanotube field emitters. They are robust and operate well in high vacuums unlike other field emission tips, which require ultra high vacuums (10^{-9} Torr) for successful operation.

2.3 Field emission results

Figure 6 shows preliminary field emission curves for some of the samples tested. It is well known that the ideal field emission phenomenon follows the Fowler-Nordheim prediction as given below.

$$\ln\left(\frac{I}{V^2}\right) = \ln(a) - \frac{b}{V} ; \qquad (1)$$

Where, I: emission current in amperes, V: biasing voltage in volts, and a, b are constants, which can be calculated using the following relations.

$$a = 1.54 \times 10^{-6}\left(\frac{\gamma^2 A_{(e)}}{\phi \cdot d^2}\right); \qquad b = 6.8 \times 10^7\left(\frac{\phi^{3/2} \cdot d}{\gamma}\right) \qquad (2)$$

Where, γ = the field enhancement factor, $A_{(e)}$ = actual emission area (cm²), φ = work function (eV) and d = gap between the anode and the tip (μm). Eq. (1) represents a line of the form $y = mx + c$, if $\ln (I / V^2)$ is plotted versus $1 / V$. This is called a Fowler-Nordheim (F-N) curve and is shown as an inset in Fig. 6 corresponding to the samples reported here. The linearity of these curves indicates field emission. By measuring the slope and the ordinate intercept of these F-N plots, one can calculate the constants a and b of eq. (1). This is important because by knowing a and b we can compute the actual emission area and the field enhancement factor for a give field emitter if we know the values of φ and d. This information is necessary to estimate the homogeneity of emission from a sample as explained further down in connection with hot spots of emission. The curves in Fig. 6 do not exhibit a smooth behavior according eq. (1). This is because of two reasons- (1) the sample area has tubes of varying heights confined to a certain distribution, as a result of which the threshold voltage for the whole sample actually follows a range rather than a single value, (2) the field emission is affected by the adsorbed impurities which locally decrease the work function, thus causing a lower threshold fields at some points than others as reported elsewhere[11]. The latter is a dynamic quantity, which as the test progresses and the nanotube gets hot, changes in value due to the desorption of impurities from the tube surface.
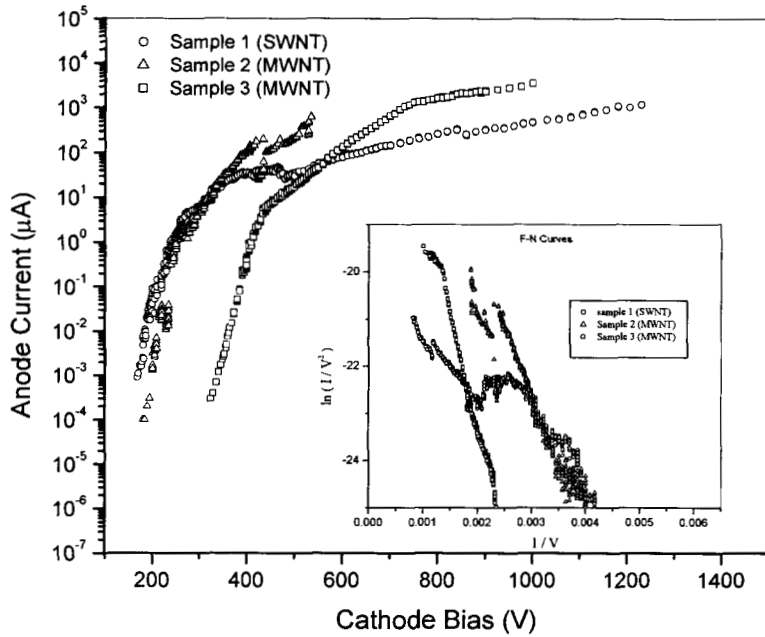
Fig. 6. Field emission curves for SWNTs and MWNTs (two samples) shown at the actual tested voltage biases. The anode-cathode gaps were ~ 40 μm, 150 μm and 160 μm respectively. The inset shows the Fowler-Nordheim curves.

Summarizing the results from Fig. 6, the highest emission currents were measured from disordered, less dense MWNTs and were found to be ~0.63 mA @ 3.6 V/μm (sample 2) and ~3.55 mA @ 6.25 V/μm (sample 3). SWNTs showed a maximum current of ~1.18 mA at 30.7 V/μm (sample 1). This low emission current from the SWNTs can be attributed to very low nanotube density in the sample area. The high density vertically aligned MWNTs (vertically aligned because of the high packing density), showed low field emission as predicted: 0.31 mA @ 4.7 V/μm. The maximum currents reported here are taken at a point beyond which it was not possible to conduct the experiment correctly owing to arcing. It was observed that, over time, all samples exhibited large variations of emission current at fixed voltage.

For the MWNT samples at certain higher fields (> 5 V/μm), the range of current variation from maxima to minima was as high as 60%.

A repeatability test was conducted on a two different samples of MWNTs, one grown using iron catalyst and the other grown using nickel catalyst, to assess the extent of variation of the emission current at a given voltage over a period of time and over ten different cycles. The results are shown in Fig. 7. At a field value of 7.65 V/μm for the first sample, the average emission was ~ 21.7 μA, which deviated ~ 9.3% over ten cycles. The same were 16.1 μA and 13.2% for the second sample. It was observed that the average value of emission current for a given field was influenced by the rate at which the field was attained. A rapid increase in the biasing voltage decreased the average emission by 2-3 %. This points to the fact that
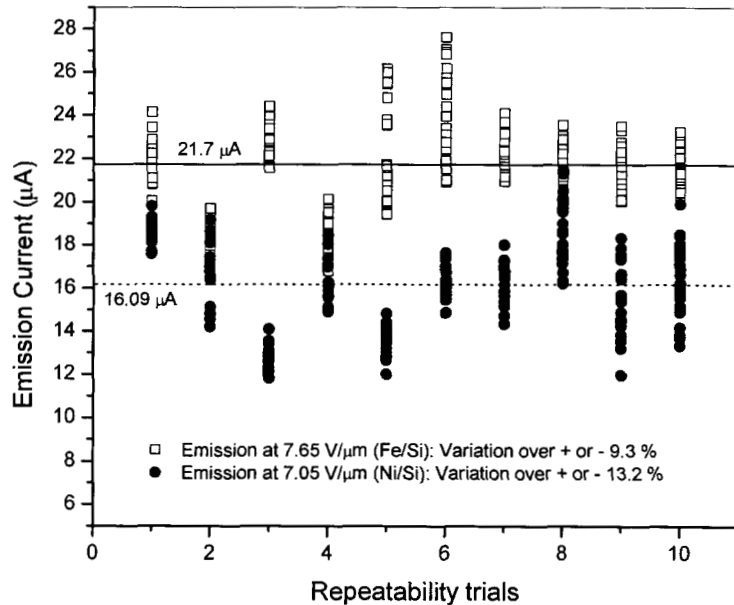

Fig. 7. Repeatability test data over ten cycles

some of the tubes may have been passed over from participating in emission by a rapid increase in the biasing field, although exact reasons are unknown at this point.

3. DISCUSSION

Although individual carbon nanotubes are capable of delivering > 30 nA of current, a closely packed sample of nanotubes do not scale up the total emission current as the number of tubes times the current per tube. This has been reported previously[12, 13], and this is because of the electrostatic screening effect that allows only a few tubes to participate in emission. On a given sample the heights of nanotubes are not equal but vary over a range. The field concentration takes place on taller tubes, which cause electrostatic screening of the surrounding shorter ones. As a result in a densely packed sample, most of the tubes lack enough field penetration to participate in field emission. It was shown elsewhere[12] that the optimum packing density of nanotubes to achieve maximum field penetration is when the inter-tube spacing is twice that of the height of the tubes. Even though an entire sample is under the influence of the field, the electrostatic screening effect causes only a few sites to field emit. These sites are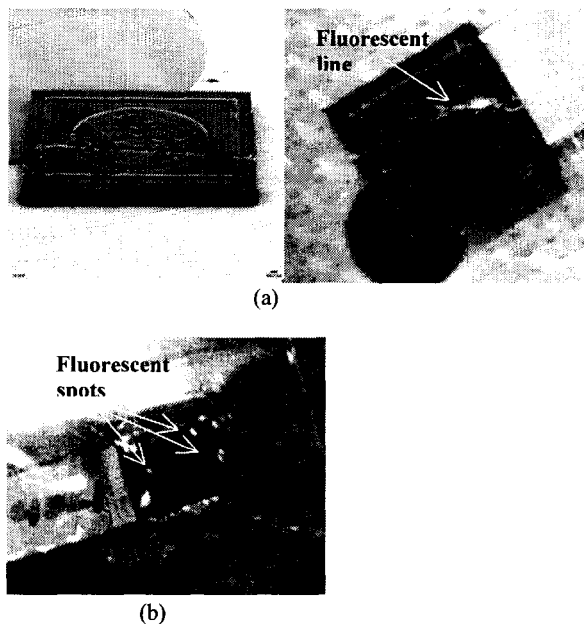 seen as "hot spots," and such hot spots can be easily identified using a global anode such as the one used here. Figure 8 (a) and (b) show optical images of fluorescent spots on the phosphor-coated anode, which correspond to the emission sites on two of the MWNT samples placed underneath. The fluorescent spot in 8 (a) corresponds to a scratch on the sample that was made to study this point. The scratch on the sample modified the tube density at that region isolating a set of tubes from the bulk thus causing them to emit preferentially than the rest of the sample. The same is true for the sample in 8 (b). The close-up SEM micrograph of the MWNT sample in Fig. 3 (b) corresponds to the sample in 8 (b). It shows slightly bent nanotubes at one of the peripheries. Few such spots existed on that sample and they can be identified as fluorescent spots in 8 (b). This effect is even better illustrated by estimating, within reasonable approximations, the actual number of nanotubes taking part in emission that cause those spots. This can be done by computing the emission area using the corresponding F-N curve and the eq. (2). The sample in Fig. 8 (b) corresponds to sample 3 of Fig. 6. By fitting the corresponding F-N curve, parameters a and b were deduced to be 1.98×10^{-6} and 5,257. An anode-cathode gap of $\sim$ 160 μm (= d) was used for this sample. Using a work function value of $\sim$ 4.5 eV (= ϕ), and solving for $A_{(e)}$, we get 3.79×10^{-14} m^2. A single MWNT in sample 3 measures $\sim$ 50 nm in diameter. By fitting such tubes into the above calculated emission area, a mere 19 nanotubes are estimated to be participating in field emission! This is incredibly low compared to several billions of tubes that are present in the sample area. This clearly indicates that by increasing the emission efficiency (number of tubes emitting per unit area), a very high current density- on the order of hundreds of amperes- can be achieved.

(a)

(b)

Fig. 8. Fluorescence on the anode, corresponding to emission sites on CNT samples, shows spotty and scattered field emission.

One of the parameters that dictate the emission performance of nanotubes is the field value, which is dictated by the anode-cathode gap. It is important to note that the physically set gap is not exactly equal to the actual gap when the biasing voltage is applied. It has been observed that, during measurements, the electrostatic force tends to unfurl nanotubes and stand them up thus decreasing the effective gap. A correction will have to be applied if the physical gap is comparable to the nanotubes lengths.
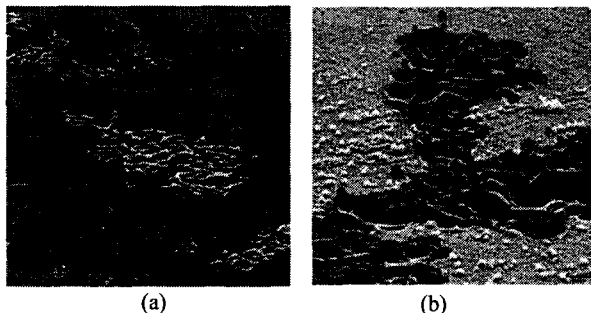

(a)   (b)

Fig. 9. Damaged CNT sample surface due to high field effects.
The nanotubes have been thrown off due to surface erosion.

On a final note, the samples that were tested at very high fields experienced failure due to electric arcing as well as due to the forced removal of nanotubes from the sample surface. Effect of high fields can be seen in Figure 9 (a) and (b). The SEM micrographs show explosive erosion of nanotubes from the sample surface and melted spots.

ACKNOWLEDGMENTS

REFERENCES

1. A.A. Talin, K.A. Dean, and J.E. Jaskie, "Field emission displays: a critical review," *Solid-State Electronics*, **45**, 963-976, 2001

2. J.M. Bonard., H. Kind, T. Stöckli, and L.-O. Nilsson, "Field emission from carbon nanotubes: the first five years," *Solid-State Electronics*, **45**, 893-914, 2001

3. W.B. Choi, D.S. Chung, J.H. Kang, H.Y. Kim, Y.W. Jin, I.T. Han, Y.H. Lee, J.E. Jung, N.S. Lee, G.S. Park, and J.M. Kim, "Fully sealed, high-brightness carbon-nanotube field-emission display," *Appl. Phys. Lett.* **75** (20), 3129-3131, 1999

4. H. Murakami, M. Hirakawa, C. Tanaka, and H. Yamakawa., "Field Emission From Well-Aligned, Patterned, Carbon Nanotube Emitters" *Appl. Phys. Lett.* **76** (13), 1776-1778, 2000

5. W. Zhu, C. Bower, G.P. Kochankski, and S. Jin, "Electron field emission from nanostructured diamond and carbon nanotubes," *Solid-State Electronics*, **45**, 921-928, 2001

6. R.H. Fowler, L.W. Nordheim, *Proc. R. Soc.,* London, Ser. A **119**, 173, 1928

7. K. Matsumoto, Kinosita S, Gotoh Y, Uchiyama T, Manalis S, Quate C. *Appl. Phys. Lett.* **78** (4), 539-540, 2001

8. P.H. Siegel, T.H. Lee, J. Xu, "The Nanoklystron: A New Concept for THz Power Generation," *JPL New Technology Report*, NPO 21014, Mar. 21, 2000

9. P.H. Siegel, A. Fung, H.M. Manohara, J. Xu and B. Chang, "Nanoklystron: A Monolithic Tube Approach to THz Power Generation," *12th Int. Sym. on Space THz Tech.*, San Diego, Feb. 14-16, 2001

10. C. Bower, W. Zhu, S. Jin, and O. Zhou, "Plasma-induced alignment of carbon nanotubes," *Appl. Phys. Lett.*, **77** (6), 830-832, 2000

11. V. Semet *et al*, "Field electron emission from individual carbon nanotubes of a vertically aligned array," *Appl. Phys. Lett.*, **81** (2), 343-345, 2002

12. L. Nisson *et al*, "Scanning field emission from patterned carbon nanotube films," **76** (15), 2071-2073, 2000

13. K.B.K. Teo *et al*, "Field emission from dense, sparse, and patterned arrays of carbon nanofibers," *Appl. Phys. Lett.*, **80** (11), 2011-2013, 2002